frontiers | Frontiers in Physics

TYPE Mini Review
PUBLISHED 08 September 2025
DOI 10.3389/fphy.2025.1674248

OPEN ACCESS

EDITED BY
Xi Xia,
Shanghai Jiao Tong University, China

REVIEWED BY
Hongliang Luo,
Harbin Engineering University, China
Kun Wu,
Institute of Mechanics (CAS), China

*CORRESPONDENCE
Zehao Feng,
fengzehao@ujs.edu.cn

RECEIVED 27 July 2025
ACCEPTED 13 August 2025
PUBLISHED 08 September 2025

CITATION
He C, Feng Z, Zhang Z and He Z (2025) Applications of jet–jet/film impingement for atomization enhancement.
Front. Phys. 13:1674248.
doi: 10.3389/fphy.2025.1674248

Applications of jet–jet/film impingement for atomization enhancement

Chengming He[1], Zehao Feng[1]*, Zhenyu Zhang[2,3] and Zhixia He[1]

[1]Institute for Energy Research, Jiangsu University, Zhenjiang, China, [2]National Key Laboratory of Multi-perch Vehicle Propulsion Systems, Beijing, China, [3]School of Mechanical Engineering, Beijing Institute of Technology, Beijing, China

This mini-review mainly focuses on the fundamental problem of jet–jet/film impingement exhibiting superior fragmentation and atomization characteristics compared to single-jet injection; this has been widely used in agricultural irrigation and combustion propulsion systems. First, it presents the main controlling parameters and spray characteristic for both jet–jet and jet–film configurations, analyzes the breakup mechanisms, and points out the coupling between jet fragmentation processes and collision-induced or externally imposed vorticity fields. Then, the atomization enhancement of jet–jet or jet–film impingement is explained from the aspects of vortex generation, evolution, identification, and the interactions between vorticity fields and spray fields. Finally, representative applications of jet–jet/film impingement in agricultural engineering and aerospace engineering are introduced so as to achieve spatially uniform spray distribution and efficient fuel/oxidizer mixing characteristics. Future advancements require breakthroughs in cross-scale vortex–ligament interaction diagnostics and intelligent control of variable-viscosity fluids to promote deep implementation of this technology in clean energy systems.

KEYWORDS

jet-jet/film impingement, atomization, vortex dynamics, spray injector, vortex diagnose

1 Introduction

Liquid jet atomization has been extensively used in various industrial applications, such as liquid fuel atomization and combustion in propulsion systems [1, 2], electrostatic spray coating [3], high-pressure spray aspirating in mining [4], pesticide spraying and agricultural irrigation [5, 6], fire-fighting [7], spray cooling [8], and respiratory disease treatment [9]. Liquid atomization describes the dynamic process involving the liquid jet breaking up into dispersed droplets by hydrodynamic instabilities [10, 11]. Examples are the primary breakup of liquid jet into filaments or large droplets by Kelvin–Helmholtz (KH) instability and then secondary breakup of filaments into small dispersed droplets by Rayleigh–Plateau (PR) instability or frequent droplet collision dynamics exerted by aerodynamic forces.

Compared to the direct injection of jet atomization [10, 12], jet–jet/film impingement [13] can prominently increase the gas liquid surface area and enhance atomization. Jet–jet/film impingement generally involves substantial jet deformation and the unstable breakup of a liquid sheet [14, 15] with a broad spray distribution in which the breakup mechanism is more complicated than that of single jet fragmentation.

This mini-review introduces the jet–jet/film impingement phenomenon and the spray characteristics influenced by several main controlling parameters in Section 2. The interpretation of the atomization enhancement of jet–jet/film impingement from a vortical perspective is presented in Section 3, followed by some widely used applications in agriculture and engine systems in Section 4 and suggestions for future research in Section 5.

2 Phenomenal description of jet–jet/film impingement and atomization

A typical jet–jet impingement configuration [15] is schematically shown in Figure 1a. It generally includes four main controlling parameters: jet diameter D, impact velocity vector U for each jet, impact angle 2α, and liquid viscosity μ. The entire atomization process of jet–jet impingement can be described as the formation of a thin liquid sheet upon impingement, followed by the propagation and intensification of surface capillary waves induced by the surface KH instability along the liquid sheet as well as the liquid sheet breakup [16, 17] either at the center or rim to generate a large number of ligaments or dispersed droplets once the impact velocity is sufficiently large. As it increases the impact velocity at fixed impact angle, liquid sheet formation shows five distinct regimes [18]: liquid chain, closed edge, opening edge, unstable edges, and liquid sheet breakup.

Jet–jet impingement is symmetrically mirrored [13, 19] based on the symmetry plane, leading to a nonuniform distribution of the ligament and droplet formation that is merely close to the symmetry plane. Thus, Zhang and colleagues [20] proposed misaligned impinging jets by defining a misalignment ratio e, where the droplet distribution becomes more uniform at a moderately misaligned impingement owing to the competition between enhanced mass stretching and reduced mass contact volume as increasing e. In addition, He and colleagues [14] proposed spinning jet–jet impingement by breaking the mirror symmetry to shorten the liquid sheet breakup length and promote the ligament breakup into dispersed droplets, especially for the small flow rate conditions in practical variable-flow engines [21].

Jet–film impingement [22, 23] is schematically shown in Figure 1b, with additional controlling parameters of liquid film thickness h. Again, increasing the impact velocity shows the three distinct breakup modes [22] of close arch spray, mantle sheet, and fully developed fan spray. Generally, as the jet perpendicularly impacts on the film, the spray angle [22, 24] can be approximately determined by the momentum ratio between the radial jet flow and axial film flow. Analogously, transverse jet injection (jet–gas crossflow) exhibits a characteristic "horseshoe vortex" [25] near the jet root. When the gas velocity is sufficiently close to supersonic, a bow shock [26, 27] may occur around the jet that interacts with the liquid jet breakup.

3 Vortex interpretation for jet–jet/film atomization enhancement

In practical spray environments usually involving complex turbulence flow, the liquid jet atomization process is probably strongly coupled with the evolution of the vortex field. Understanding and controlling vortices can enhance jet–jet and jet–film atomization leading to finer droplets, better mixing, and higher energy efficiency; vortex field control is thus fundamental to advancing jet–jet and jet–film atomization technologies [30].

3.1 Vortex formation, evolution, and identification of jet–jet/film impingement

When fluid flows through a nozzle, the presence of a boundary layer causes fluid molecules near the nozzle wall to move more slowly, while those away from the wall move faster, creating a velocity gradient [31–33]. As the jet exits the nozzle, shear layer instabilities cause the fluid to roll up, forming a toroidal vortex structure. There is also an obvious mushroom-shaped entrainment vortex at the jet head due to the liquid gas interaction. Vortex rings and vortex entrainment are classic coherent structures, commonly observed in free jets [34–36].

In jet–jet flow, two colliding jets interact, leading to complex vortex dynamics due to stagnation, shear, and flow instabilities [17] (Figure 1c). First, the impingement zone forms a high-pressure stagnation region, deflecting flow radially outward. Velocity gradients between the jets generate shear layers, which roll up into vortices via KH instability. If the jets are pulsed or turbulent, coherent vortex rings may form and interact upon collision [17]. Wu and colleagues [37] investigated a moderate Reynolds number (Re = 4,050) turbulent opposed jet flow by using direct numerical simulation. They analyzed the turbulent flow field by using the proper orthogonal decomposition (POD) technique and found that the first POD mode includes a vortex ring situated in the impinging zone which is capable of shifting the axial position of the stagnation point. In contrast, the second to fourth POD modes contain several vortices that rotate alternately in two directions along the radial axis, and these vortices primarily induce tilting and distortion effects on the stagnation plane. Vortex evolution and breakdown in opposed-jets flow are governed by shear layer instabilities, Reynolds number effects, and nozzle geometry, leading to primary vortex stretching, secondary vortex generation, and eventual turbulent dissipation [38].

In jet–film impingement, the jet strikes a thin liquid film or boundary layer on a surface. The impact creates a stagnation region with high pressure, forcing the fluid to spread radially outward. The high-velocity jet interacts with the slower-moving film, creating a shear layer. KH instabilities may develop, leading to roll-up vortices at the jet–film interface [39, 40]. Moreover, the radial outflow from the impingement point may form a hydraulic jump (sudden increase in film thickness). Behind the jump, vortices can form due to adverse pressure gradients. The formation and evolution of the vortices are mainly influenced by jet velocity, film thickness, impingement angle, and fuel properties. Zhang and colleagues [18] investigated the height and distance of the jet–film vortex core under different ambient pressures and cross-flow velocities using

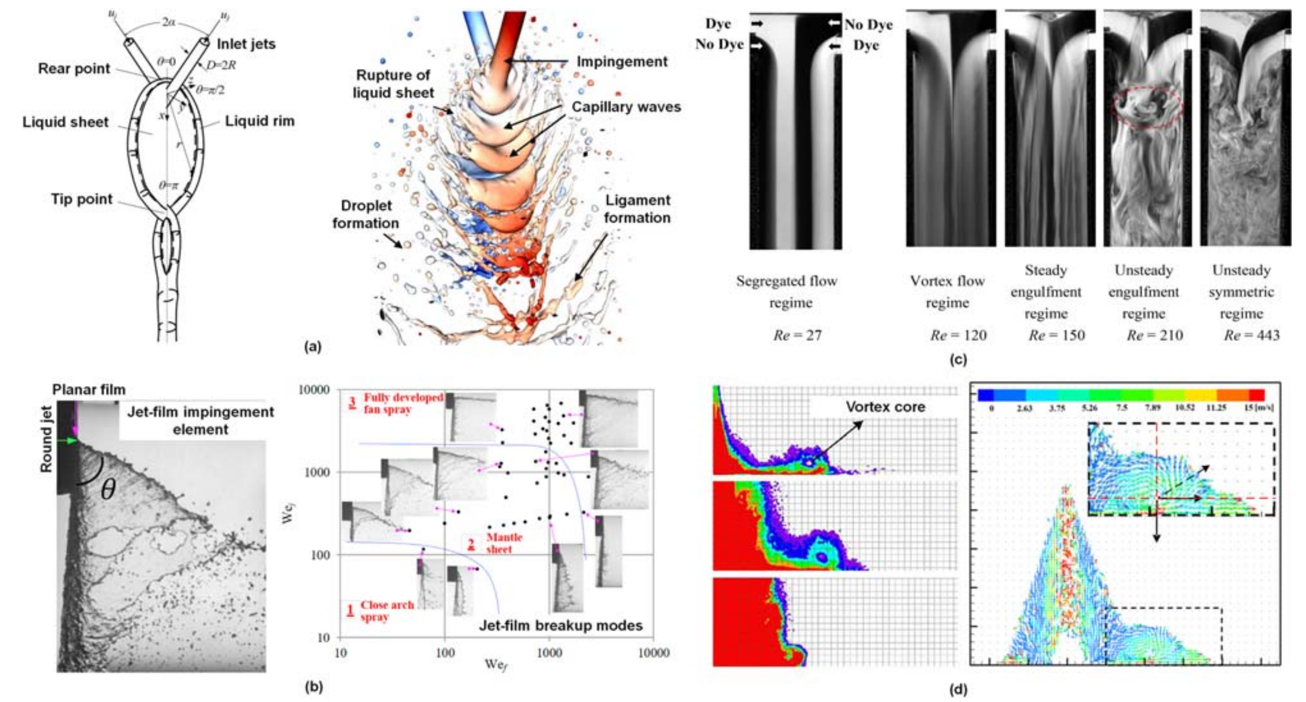

FIGURE 1
Phenomenal description of jet–jet/film impingement and atomization. **(a)** Schematic of jet–jet impingement and atomization process (adapted with permission from Chen et al. [15] Copyright 2013, Begell House Inc.); **(b)** distinct breakup modes for jet–film impingement (adapted with permission from Cheng et al. [22] Copyright 2018, Elsevier Ltd.); **(c)** vortex formation for jet–jet impingement at different Reynolds numbers (adapted with permission from Xue et al. [28] Copyright 2023, Elsevier B.V.); **(d)** vortex diagnosis using PIV technology for jet–film impingement (adapted with permission from Zhang et al. [29] Copyright 2022, Elsevier Ltd.).

laser sheet technology. An indicator of the "contribution index" was proposed to evaluate the degree of influence of different influencing factors.

With advancements in vortex dynamics research, a variety of vortex identification methods [41–43] have been developed, including the *Q*, *k*, *D*, and swirling strength criteria. These techniques play a crucial role in analyzing and understanding complex vortex structures in fluid dynamics. However, the problem of finding the best vortex identification techniques is still controversial.

3.2 Vortex diagnose technics

High-speed imaging is a widely used experimental technique for diagnosing vortex dynamics in jet–jet/film impingement studies [44, 45]. By employing ultra-fast cameras, researchers can resolve transient flow phenomena such as vortex formation, evolution, and breakdown. The technique often incorporates tracer particles or fluorescent dyes for enhanced contrast, combined with backlight illumination or laser sheet lighting to clearly visualize thin film dynamics (radial spreading, hydraulic jumps, and vortex roll-up) and interfacial instabilities caused by jet–jet/film interactions [5, 38].

For the quantitative measurement of instantaneous velocity fields, particle image velocimetry (PIV) is a powerful non-intrusive flow diagnostic technique. By illuminating seeded tracer particles with a pulsed laser sheet and capturing their displacements via synchronized high-speed cameras, PIV provides two- (2D-PIV) or three-component (3D stereoscopic/volumetric PIV) velocity vector maps of the flow field [46, 47]. In jet–jet/film impingement research, PIV enables the precise characterization of vortex dynamics through derived quantities like vorticity, swirling strength, and *Q*-criteria, revealing key features such as shear layer roll-up, recirculation zones, and vortex-ring structures (Figure 1d).

Modern advances like tomographic PIV (Tomo-PIV) can reconstruct 3D vortex tubes and coherent structures [48], while microscopic PIV (μPIV) resolves near-wall phenomena [49]. When combined with machine-learning-assisted diagnostics, PIV data can effectively identify dominant vortex modes [50]. This makes it an indispensable tool for validating CFD models and understanding complex vortex interactions.

3.3 Interaction between vortex field and spray characteristics

The interaction between jet–jet/film vortex fields and spray characteristics represents a complex multiphase phenomenon where coherent vortical structures fundamentally govern spray development and atomization processes [51, 52]. In dual-jet impingement or jet–film interaction systems, the collision and merging of vortex filaments from adjacent jets create intricate three-dimensional flow topologies that dramatically alter spray formation. Wang and colleagues [53] compared the hydraulic performance between jet-impingement and non-impinging sprinklers by using highspeed photography (HSP). Their results show that the developed jet impingement sprinkler achieved a smoother water distribution trend.

The primary vortex dynamics include shear layer roll-up from individual jets, collision-induced vortex pairing, and film-driven recirculation zones which collectively control the liquid breakup mechanism through several interconnected pathways. Large-scale vortex rings generated at jet boundaries enhance primary atomization by extruding liquid sheets and promoting Rayleigh–Taylor instabilities, while small-scale turbulent vortices in the merging region drive secondary droplet fragmentation through intense velocity fluctuations [54]. Xia and colleagues [55] found that a type of large scale instability due to a vortex ring located at the impingement zone promotes the breakup of the water sheet or ligaments, forming smaller droplets. Moreover, coherent vortices entrain droplets, altering trajectories and enhancing radial/axial spreading. These vortices preferentially transport larger droplets toward the spray periphery through centrifugal effects while simultaneously promoting more homogeneous mixing of droplet sizes [56].

In propulsion systems, these vortex-mediated spray patterns directly affect combustion stability [57], while in industrial coating applications and agricultural production applications they determine deposition uniformity [58–60]. Current research is focused on active flow control strategies to manipulate vortex interactions for optimized spray performance across different Weber and Reynolds number regimes, although the nonlinear coupling between vortex merging dynamics and droplet formation pathways remains a key challenge in predictive modeling.

4 Applications of jet–jet/film impingement

The application of sprinklers [53, 61, 67–70] in agricultural engineering (Figure 2a) adopts the asymmetric impingement between a primary and a secondary jet to replace the traditional single water-jet-dispersing devices in rotating sprinklers [71–73] and promote atomized performance, especially for low-pressure conditions [32, 67, 74]. Jiang and colleagues [61] found the Christiansen's uniformity coefficient [75] of the jet impingement sprinkler with various elevation angles of secondary nozzle greater than the non-impingement sprinkler. Many parameter optimization studies have demonstrated that the nozzle geometry [34, 51, 76, 77], angle of dispersion [78], aspect ratio [34, 79], and aperture ratio [53, 80] for the primary and secondary jets can significantly influence jet instabilities and breakup characteristics in agricultural irrigation.

Apart from jet–jet impingement, some other jet-based methods can also be used in sprinklers to adapt hydraulic performance. Fan-type nozzles [54, 62, 81] increase the total liquid surface area to facilitate atomization [82] by forming a fan-shaped liquid sheet (Figure 2b), while the penetration distance of the liquid sheet is generally smaller than the jet–jet impingement. For oil-based emulsion spray [81, 83, 84], the holes and web structures [62, 85, 86] break up the inner liquid sheet differently from the water liquid sheet, generally showing the rim breakup. For larger liquid viscosity, the enhanced viscous dissipation would suppress surface capillary wave propagation and subsequent liquid sheet breakup. In addition, non-Newtonian jet–jet impingement [7, 87] and two miscible liquid jets with different surface tensions [85] would further complicate the breakup mechanism [88] and enrich the breakup phenomenon.

An air-assisted nozzle [63, 89] can promote the liquid jet breakup owing to the large shearing effects and kinetic energy of gas (Figure 2c). The combination of air-assisted nozzle and electrostatic excitation [5, 63, 90] can further promote atomization and reduce the need for pesticide spraying. In addition, as shown in Figure 2d, the atomization of a traditional sprinkler can be developed by using a driving arm [64] to cut the water jet periodically with appropriate driving frequency and injection pressure. Similarly, as shown in Figure 2e, a dispersion tooth inserted into the water jet [65, 91, 92] has been shown to be an effective way of improving the uniformity of water distribution from irrigation sprinklers.

For applications in high-thrust rocket engines [13, 93] and opposed-piston compression ignition engines (CIE) [94, 95], liquid fuel atomization and subsequent spray combustion would be substantially enhanced owing to the promoted droplet collision probability (Figure 2f). The impingement is a direct and efficient way to promote the atomization of heavy oil or bio-oil [96, 97]. In addition, for the pintle injector [24, 25, 66, 98] utilized in the applications of variable-thrust rocket engines, the spray cone is formed by the radial jet flow impinging the axial annular film flow, which has a simple structure, continuous flow regulation, and stable combustion superior to other variable-thrust methods.

The phenomenon of jet–jet impingement in agricultural irrigation should not be essentially different from that in combustion systems once the dynamic similarities are satisfied with approximately dimensional parameters. For example, jet–jet/film breakup is generally controlled by two important parameters: the Weber number $We = \rho D U^2/\sigma$ (ρ is the liquid density, D the jet diameter, U the relative velocity, and σ the surface tension coefficient) measures the relative importance of the jet impact inertia compared to the surface tension; the Ohnesorge number $Oh = \mu/\sqrt{\rho D \sigma}$ (μ is the liquid viscosity) represents the relative importance of the viscous force to impact inertia and surface tension. A larger jet diameter in agricultural irrigation generally leads to a larger We or a smaller Oh, which is approximately equivalent to an increase of jet impact velocity or a decrease of liquid viscosity promoting the development of jet instabilities and subsequent jet breakup. However, the dispersed droplet size in agricultural irrigation would be larger than that in combustion systems owing to its initial sufficiently large jet diameter.

In addition, the internal cavitation [99, 100] of various nozzles is also a significant factor influencing the flow rate and external jet atomization in agriculture [101]; this is the same in combustion systems that influence the combustion emission characteristics [102, 103] based on dual-fuel direct injection [103].

5 Discussion and concluding remarks

For jet–jet impingement at given fluid property and impact angle, the most direct and straightforward way to enhance atomization is to increase the impingement velocity. However, in practical applications of fuel injection in engines, achieving higher

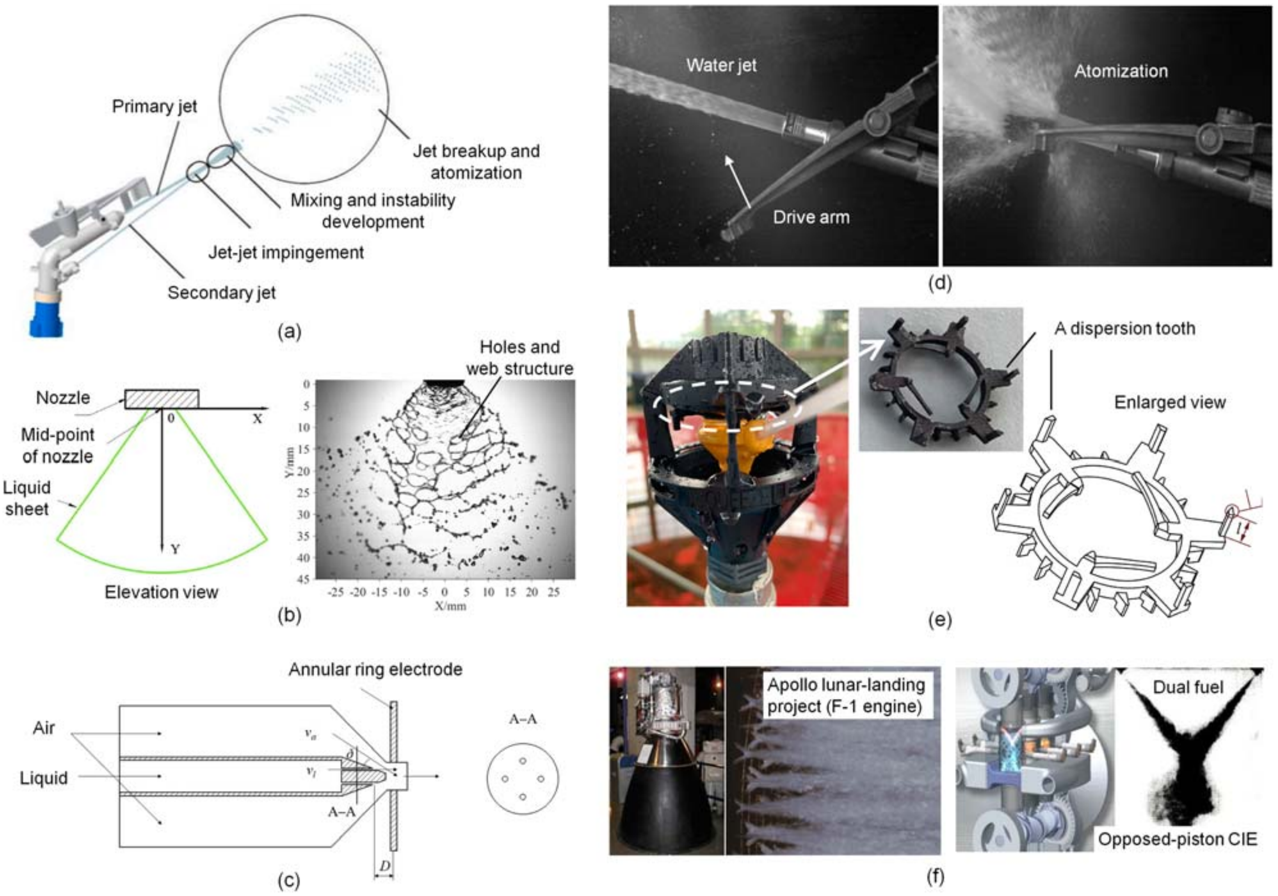

FIGURE 2
Applications of jet–jet/film impingement in agriculture and propulsion engines. **(a)** The sprinkler involves a primary jet impacting with a secondary jet (adapted with permission from Jiang et al. [61] Copyright 2024, by Elsevier Ltd.); **(b)** fan-type nozzles of a fan-shaped liquid sheet (adapted with permission from Gong et al. [62] Copyright 2020, by Elsevier Ltd.); **(c)** air-assisted nozzle (adapted with permission from Dai et al. [63] Copyright 2017, The Authors); **(d)** atomization enhancement by a driving arm (adapted with permission from Tang and Chen [64] Copyright 2022, The Authors); **(e)** liquid jet impinging a dispersion tooth (adapted with permission from Pan et al. [65] Copyright 2024, by Elsevier Ltd.); **(f)** pintle injector of jet–film impingement (adapted with permission from Zhao et al. [66] Copyright 2022 by Elsevier Ltd.).

injection velocities usually requires a sufficiently large injection pressure drop which negatively impacts economic efficiency and implementation feasibility owing to the difficulty of creating such a large injection pressure drop. In addition, for variable-thrust engines at low throttling levels, the injection velocities cannot be sufficiently high. Thus, alternative injection strategies—such as swirl injection or off-center impingement-to-break symmetry—could be employed to attain desirable spray enhancement.

For jet–film impingement, decreasing film thickness leads to worse spray characteristics with increased spray angle and enhanced nonuniformity of droplet distribution—indicating that the atomization is dominated by the local effective impact between jet and film. Jet–jet impingement generally has better atomization than jet–film impingement owing to sufficient impact; however, the jet–film injection element is still widely and successfully used in pintle injectors in variable-thrust rocket engines because its mixing characteristics between fuel and oxidizer is better than jet–jet impingement, although atomization plays a secondary role in combustion when the combustor is sufficient large for complete combustion.

Jet–jet/film impingement for atomization enhancement has been widely applied in agriculture and propulsion systems. The most crucial factor causing liquid jet atomization is generating and magnifying the non-uniformity induced by such as hydrodynamic instabilities, local-strain-rate-dependent non-Newtonian fluid, gelled propellants, or exerted in an external electromagnetic field. In addition, it is essential to fully exploit interactions between the external flow field and droplets, thereby regulating energy transfer between hydrodynamic instabilities and external vortical structures. This enables precise control over the spatial distribution and droplet size of atomization characteristics.

The roles of various hydrodynamic instabilities and possible competition among the impact inertia, surface tension, and viscosity of various liquid jets in affecting jet–jet/film breakup and atomization characteristics are strongly coupled so that it is difficult to obtain a general design principle by focusing on only one parameter at a time. Fortunately, artificial intelligence (AI) techniques and machine learning algorithms in agriculture [104–107] could be very powerful for jet/film breakup prediction models by importing various experimental data to address the prediction bottleneck of traditional physical models in strongly nonlinear, multi-scale scenarios; this merits extensive future study.

Author contributions

CH: Conceptualization, Formal Analysis, Writing – review and editing, Writing – original draft. ZF: Writing – review and editing, Investigation, Writing – original draft. ZZ: Project administration, Supervision, Writing – review and editing. ZH: Writing – review and editing, Funding acquisition, Supervision.

Funding

The author(s) declare that financial support was received for the research and/or publication of this article. The authors acknowledge the Open Foundation of National Key Laboratory of Multi-perch Vehicle Propulsion Systems (QDXT-WY-202407-11) from the Beijing Institute of Technology.

Acknowledgments

The authors acknowledge the Open Foundation of National Key Laboratory of Multi-perch Vehicle Propulsion Systems (QDXT-WY-202407-11) from the Beijing Institute of Technology.

Conflict of interest

The authors declare that the research was conducted in the absence of any commercial or financial relationships that could be construed as a potential conflict of interest.

Generative AI statement

The author(s) declare that no Generative AI was used in the creation of this manuscript.

Any alternative text (alt text) provided alongside figures in this article has been generated by Frontiers with the support of artificial intelligence and reasonable efforts have been made to ensure accuracy, including review by the authors wherever possible. If you identify any issues, please contact us.

Publisher's note

All claims expressed in this article are solely those of the authors and do not necessarily represent those of their affiliated organizations, or those of the publisher, the editors and the reviewers. Any product that may be evaluated in this article, or claim that may be made by its manufacturer, is not guaranteed or endorsed by the publisher.

References

1. Ashgriz N. *Handbook of atomization and sprays: theory and applications*. New York, NY: Springer Science and Business Media (2011).

2. Sirignano WA. *Fluid dynamics and transport of droplets and sprays*. Cambridge: Cambridge University Press (2010).

3. Law SE. Agricultural electrostatic spray application: a review of significant research and development during the 20th century. *J Electrost* (2001) 51:25–42. doi:10.1016/S0304-3886(01)00040-7

4. Huang R, Tao Y, Chen J, Li S, Wang S. Review on dust control technologies in coal mines of China. *Sustainability* (2024) 16(10):4038. doi:10.3390/su16104038

5. Appah S, Wang P, Ou M, Gong C, Jia W. Review of electrostatic system parameters, charged droplets characteristics and substrate impact behavior from pesticides spraying. *Int J Agric Biol Eng* (2019) 12(2):1–9. doi:10.25165/j.ijabe.20191202.4673

6. Talaviya T, Shah D, Patel N, Yagnik H, Shah M. Implementation of artificial intelligence in agriculture for optimisation of irrigation and application of pesticides and herbicides. *AI Agric* (2020) 4:58–73. doi:10.1016/j.aiia.2020.04.002

7. Rohilla M, Saxena A, Dixit PK, Mishra GK, Narang R. Aerosol forming compositions for fire fighting applications: a review. *Fire Technol* (2019) 55(6):2515–45. doi:10.1007/s10694-019-00843-7

8. Cheng W-L, Zhang W-W, Chen H, Hu L. Spray cooling and flash evaporation cooling: the current development and application. *Renew Sust Energ Rev* (2016) 55:614–28. doi:10.1016/j.rser.2015.11.014

9. Feng X, Shi Y, Zhang Y, Lei F, Ren R, Tang X. Opportunities and challenges for inhalable nanomedicine formulations in respiratory diseases: a review. *Int J Nanomed* (2024) 19:1509–38. doi:10.2147/ijn.s446919

10. Eggers J, Villermaux E. Physics of liquid jets. *Rep Prog Phys* (2008) 71(3):036601. doi:10.1088/0034-4885/71/3/036601

11. Li Y, Zhu M, Wu K, Liu D, Xi R. Theoretical study on the interfacial instability of a spherical droplet subject to vertical vibration. *Phys Fluids* (2024) 36(1):012123. doi:10.1063/5.0187412

12. Hasslberger J, Ketterl S, Klein M, Chakraborty N. Flow topologies in primary atomization of liquid jets: a direct numerical simulation analysis. *J Fluid Mech* (2019) 859:819–38. doi:10.1017/jfm.2018.845

13. Chen X, Yang V. Recent advances in physical understanding and quantitative prediction of impinging-jet dynamics and atomization. *Chin J. Aeronaut* (2019) 32(1):45–57. doi:10.1016/j.cja.2018.10.010

14. He C, Zhu F, Chen H, Ji H, He Z. Enhancement of liquid sheet breakup and atomization for spinning jet–jet impingement. *Phys Fluids* (2025) 37(2):022141. doi:10.1063/5.0256566

15. Chen X, Ma D, Yang V, Popinet S. High-fidelity simulations of impinging jet atomization. *Atomization sprays* (2013) 23(12):1079–101. doi:10.1615/atomizspr.2013007619

16. Yang L-J, Zhao F, Fu Q-F, Cui K-D Liquid sheet formed by impingement of two viscous jets. *J Propul Power* (2014) 30(4):1016–26. doi:10.2514/1.b35105

17. Xie Y, Zhang J, Sun M, Wu J, Li P, An B, et al. Review on spray characteristics of liquid–liquid injectors in liquid rocket engines. *Phys Fluids* (2024) 36(9):091302. doi:10.1063/5.0223894

18. Bush JW, Hasha AE. On the collision of laminar jets: fluid chains and fishbones. *J Fluid Mech* (2004) 511:285–310. doi:10.1017/s002211200400967x

19. He C, He Z, Zhang P. Droplet collision of hypergolic propellants. *Droplet* (2024) 3(2):e116. doi:10.1002/dro2.116

20. Zhang C, Zhang Z, Wu K, Xia X, Fan X. Atomization of misaligned impinging liquid jets. *Phys Fluids* (2021) 33(9):093311. doi:10.1063/5.0061981

21. He C, Luo W, Zhang P, He Z, Yue L. Spray combustion characteristics of a gas–liquid pintle injector with variable swirl intensities. *Phys Fluids* (2023) 35(9):097111. doi:10.1063/5.0164130

22. Cheng P, Li Q, Chen H. Flow characteristics of a pintle injector element. *Acta Astronaut.* (2019) 154:61–6. doi:10.1016/j.actaastro.2018.10.020

23. He C, Zhang P, He Z, Yue L. Analysis of spray characteristics of a jet-film injection element based on Voronoi tessellation. *Acta Astronaut.* (2023) 206:100–13. doi:10.1016/j.actaastro.2023.02.006

24. Zhao F, Zhang H, Zhao L, Bai B. A new modeling method for spray angle prediction of liquid–liquid pintle injector. *AIAA J* (2023) 61(11):4960–75. doi:10.2514/1.j063068

25. Xiao Y, Zhang H, Chen Z, Zhang H, Zheng C. Numerical investigation on the transverse jet into a supersonic crossflow with different pressure ratios. *Eng Appl Comput Fluid Mech* (2024) 18(1):2354760. doi:10.1080/19942060.2024.2354760

26. Huh J, Lee S. Numerical study on lateral jet interaction in supersonic crossflows. *Aerosp Sci Technol* (2018) 80:315–28. doi:10.1016/j.ast.2018.07.022

27. Liang C-H, Sun M-B, Liu Y, Li G-X, Yu J-F. Numerical study of flow structures and mixing characteristics of a sonic jet in supersonic crossflow. *Acta Astronaut.* (2020) 166:78–88. doi:10.1016/j.actaastro.2019.10.008

28. Xue L, Liu G, Wang Y, Hao Z, Bie H. Vortex shedding of unsteady symmetric flow regime induced by secondary impinging in T-T jet reactors. *J Chem Eng* (2023) 471:144468. doi:10.1016/j.cej.2023.144468

29. Zhang G, Si Z, Zhai C, Luo H, Ogata Y, Nishida K. Characteristics of wall-jet vortex development during fuel spray impinging on flat-wall under cross-flow conditions. *Fuel* (2022) 317:123507. doi:10.1016/j.fuel.2022.123507

30. Kaplanski F, Sazhin SS, Begg S, Fukumoto Y, Heikal M. Dynamics of vortex rings and spray-induced vortex ring-like structures. *Eur J Mech B Fluids* (2010) 29(3):208–16. doi:10.1016/j.euromechflu.2010.01.002

31. Jiang Y, Li H, Chen C, Xiang Q. Calculation and verification of formula for the range of sprinklers based on jet breakup length. *Int J Agric Biol Eng* (2018) 11(1):49–57. doi:10.25165/j.ijabe.20181101.2777

32. Jiang Y, Li H, Hua L, Zhang D, Issaka Z. Experimental study on jet breakup morphologies and jet characteristic parameters of non-circular nozzles under low-intermediate pressures. *Appl Eng Agric* (2019) 35(4):617–32. doi:10.13031/aea.13291

33. Lin H, Li H, Jiang Y. Axis-switching behavior of liquid jets issued from non-circular nozzles under low-intermediate pressure. *Appl Eng Agric* (1997) 37(2):367–78. doi:10.13031/aea.14245

34. Jiang Y, Li H, Chen C, Hua L, Zhang D. Hydraulic performance and jet breakup characteristics of the impact sprinkler with circular and non-circular nozzles. *Appl Eng Agric* (2019) 35(6):911–24. doi:10.13031/aea.13268

35. Li A, Li G, Ruan Y, Kang C, Wang R, Lu X. Research progress of kidney vortex and its application in film cooling. *Int J Heat Fluid Flow* (2025) 112:109706. doi:10.1016/j.ijheatfluidflow.2024.109706

36. Shi M, Ruan Y, Wu B, Ye Z, Zhu S. Performance evaluation of Hydrodynamic Vortex Separator at different hydraulic retention times applied in Recirculating Biofloc Technology system. *Trans ASABE* (2017) 60(5):1737–47. doi:10.13031/trans.12415

37. Wu D, Li J, Liu Z, Xiong Y, Zheng C, Medwell PR. Eulerian and Lagrangian stagnation plane behavior of moderate Reynolds number round opposed-jets flow. *Comput Fluids* (2016) 133:116–28. doi:10.1016/j.compfluid.2016.05.001

38. Li WF, Yao TL, Wang FC. Study on factors influencing stagnation point offset of turbulent opposed jets. *AIChE* (2010) 56(10):2513–22. doi:10.1002/aic.12188

39. Gong C, Jia F, Kang C. Deposition of water and emulsion hollow droplets on hydrophilic and hydrophobic surfaces. *Agriculture* (2024) 14(6):960. doi:10.3390/agriculture14060960

40. Uddin N, Kee PTW, Weigand B. Heat transfer by jet impingement: a review of heat transfer correlations and high-fidelity simulations. *Appl Therm Eng* (2024) 257:124258. doi:10.1016/j.applthermaleng.2024.124258

41. Chong M, Perry A, Cantwell B. A general classification of three-dimensional flow fields. *Phys Fluids* (1990) 2:765–77. doi:10.1063/1.857730

42. Jeong J, Hussain F. On the identification of a vortex. *J Fluid Mech* (1995) 285:69–94. doi:10.1017/s0022112095000462

43. Zhou J, Adrian RJ, Balachandar S, Kendall TM. Mechanisms for generating coherent packets of hairpin vortices in channel flow. *J Fluid Mech* (1999) 387:353–96. doi:10.1017/s002211209900467x

44. Appah S, Jia W, Ou M, Wang P, Gong C. Investigation of optimum applied voltage, liquid flow pressure, and spraying height for pesticide application by induction charging. *Appl Eng Agric* (2019) 35(5):795–804. doi:10.13031/aea.13358

45. Sun J, Lu X, Mao H, Jin X, Wu X. A method for rapid identification of rice Origin by hyperspectral imaging technology. *J Food Process Eng* (2015) 40(1):e12297. doi:10.1111/jfpe.12297

46. Ansaripour M, Dafsari RA, Yu S-H, Choi Y, Lee J. Characteristics of a tip-vortex generated by a single rotor used in agricultural spraying drone. *Exp Therm Fluid Sci* (2023) 149:110995. doi:10.1016/j.expthermflusci.2023.110995

47. Jiang Y, Li H, Xiang Q, Chen C. Comparison of PIV experiment and numerical simulation on the velocity distribution of intermediate pressure jets with different nozzle parameters. *Irrig Drain* (2017) 66(4):510–9. doi:10.1002/ird.2133

48. Hamdi J, Assoum HH, Alkheir M, Abed-Meraïm K, Cauet S, Sakout A. Analysis of the 3D flow of an impinging jet on a slotted plate using TR-Tomo PIV and Proper Orthogonal Decomposition. *Energy Rep* (2020) 6:158–63. doi:10.1016/j.egyr.2020.11.269

49. Won Y, Wang EN, Goodson KE, Kenny TW. 3-D visualization of flow in microscale jet impingement systems. *Int J Therm Sci* (2011) 50(3):325–31. doi:10.1016/j.ijthermalsci.2010.08.005

50. Giurgiu V, Beckedorff L, Caridi GCA, Lagemann C, Soldati A. Machine learning-enhanced PIV for analyzing microfiber-wall turbulence interactions. *Int J Multiph Flow* (2024) 181:105021. doi:10.1016/j.ijmultiphaseflow.2024.105021

51. Jiang Y, Li H, Hua L, Zhang D. Three-dimensional flow breakup characteristics of a circular jet with different nozzle geometries. *Biosyst Eng* (2020) 193:216–31. doi:10.1016/j.biosystemseng.2020.03.003

52. Liang Y, Tang Z, Zhang H, Li Y, Ding Z, Su Z. Cross-flow fan on multi-dimensional airflow field of air screen cleaning system for rice grain. *Int J Agric Biol Eng* (2022) 15(4):223–35. doi:10.25165/j.ijabe.20221504.6949

53. Wang Z, Jiang Y, Li H, Wang L. Enhancing hydraulic efficiency in jet impingement sprinklers: comparative analysis of aperture ratios compared with non-impingement sprinklers. *Biosyst Eng* (2024) 248:162–76. doi:10.1016/j.biosystemseng.2024.10.004

54. Gong C, Li D, Kang C. Visualization of the evolution of bubbles in the spray sheet discharged from the air-induction nozzle. *Pest Manag Sci* (2022) 78(5):1850–60. doi:10.1002/ps.6803

55. Xia Y, Khezzar L, Alshehhi M, Hardalupas Y. Atomization of impinging opposed water jets interacting with an air jet. *Exp Therm Fluid Sci* (2018) 93:11–22. doi:10.1016/j.expthermflusci.2017.12.010

56. Feng Z, Zhang J, Gu J, Jin Y, Tian X, He Z. Spatial distribution characteristics of droplet size and velocity in a methanol spray. *Processes* (2025) 13(6):1883. doi:10.3390/pr13061883

57. Barbieri MR, Achelis L, Fritsching U. Spray characteristics of steam-assisted oil atomization in Y-jet nozzles. *Int J Multiph Flow* (2024) 181:105028. doi:10.1016/j.ijmultiphaseflow.2024.105028

58. Anagri A, Baitukha A, Pulpytel J, Mori S, Arefi-Khonsari F. Double tube configuration of atmospheric pressure plasma jet for deposition of organic coatings in open air. *Chem Eng Res Des* (2024) 210:445–51. doi:10.1016/j.cherd.2024.09.006

59. Wu S, Liu J, Wang J, Hao D, Wang R. The motion of strawberry leaves in an air-assisted spray field and its influence on droplet deposition. *Trans ASABE* (2021) 64(1):83–93. doi:10.13031/trans.14143

60. Xi T, Li C, Qiu W, Wang H, Lv X, Han C, et al. Droplet deposition behavior on a pear leaf surface under wind-induced vibration. *Appl Eng Agric* (2020) 36(6):913–26. doi:10.13031/aea.14031

61. Jiang Y, Wang Z, Li H, Wang L. Optimising the hydraulic performance of a jet impingement sprinkler by varying elevation angle: a Comparative study with a non-impingement sprinkler. *Biosyst Eng* (2024) 245:24–35. doi:10.1016/j.biosystemseng.2024.06.011

62. Gong C, Kang C, Jia W, Yang W, Wang Y. The effect of spray structure of oil-based emulsion spray on the droplet characteristics. *Biosyst Eng* (2020) 198:78–90. doi:10.1016/j.biosystemseng.2020.08.001

63. Dai S, Zhang J, Jia W, Ou M, Zhou H, Dong X, et al. Experimental study on the droplet size and charge-to-Mass ratio of an air-assisted electrostatic nozzle. *Agriculture* (2022) 12(6):889. doi:10.3390/agriculture12060889

64. Tang P, Chen C. An investigation of the frequency and duration of a drive spoon–dispersed water jet and its influence on the hydraulic performance of a large-volume irrigation sprinkler. *Agron* (2022) 12(9):2233. doi:10.3390/agronomy12092233

65. Pan X, Jiang Y, Li H, Hui X, Xing S. Numerical simulation of the effect of varying dispersion tooth insertion depth on the jet breakup and hydraulic performance. *Biosyst Eng* (2024) 239:98–113. doi:10.1016/j.biosystemseng.2024.02.005

66. Zhao F, Zhang H, Zhang H, Bai B, Zhao L. Review of atomization and mixing characteristics of pintle injectors. *Acta Astronaut.* (2022) 200:400–19. doi:10.1016/j.actaastro.2022.08.042

67. Xiang Q, Qureshi WA, Tunio MH, Solangi KA, Xu Z, Lakhiar IA. Low-pressure drop size distribution characterization of impact sprinkler jet nozzles with and without aeration. *Agric Water Manag* (2021) 243:106458. doi:10.1016/j.agwat.2020.106458

68. Zhu X, Chikangaise P, Shi W, Chen W-H, Yuan S. Review of intelligent sprinkler irrigation technologies for remote autonomous system. *Int J Agric Biol Eng* (2018) 11(1):23–30. doi:10.25165/j.ijabe.20181101.3557

69. Dwomoh FA, Zhu X, Fordjour A, Liu J, Yuan S, Li H. Structural design and performance characteristics of the fluidic sprinkler application technology for saving irrigation water: a review. *J Agric Eng* (2023) 54(2):1452. doi:10.4081/jae.2023.1452

70. Zhu X, Fordjour A, Agyen Dwomoh F, Kwame Lewballah J, Anim Ofosu S, Liu J, et al. Experimental study on the effects of pressure loss on uniformity, application rate and velocity on different working conditions using the dynamic fluidic sprinkler. *Heliyon* (2024) 10(5):e27140. doi:10.1016/j.heliyon.2024.e27140

71. Wang J, Song Z, Chen R, Yang T, Tian Z. Experimental study on droplet characteristics of rotating sprinklers with circular nozzles and diffuser. *Agriculture* (2022) 12(7):987. doi:10.3390/agriculture12070987

72. Pan X, Jiang Y, Li H, Zhou X. Hydraulic performance of the rotational damping sprinkler: analysis of the force acting on diffuser tooth I. *Irrig Drain* (2024) 73(1):29–49. doi:10.1002/ird.2859

73. Hussain Z, Liu J, Chauhdary JN, Zhao Y. Evaluating the effect of operating pressure, nozzle size and mounting height on droplet characteristics of rotating spray plate sprinkler. *Irrig Sci* (2024) 1–16. doi:10.1007/s00271-024-00982-y

74. Chen R, Li H, Wang J, Guo X. Analysis of droplet characteristics and kinetic energy distribution for fixed spray plate sprinkler at low working pressure. *Trans ASABE* (2021) 64(2):447–60. doi:10.13031/trans.14139

75. Xue S, Ge M, Wei F, Zhang Q. Sprinkler irrigation uniformity assessment: relational analysis of Christiansen uniformity and Distribution uniformity. *Irrig Drain* (2023) 72(4):910–21. doi:10.1002/ird.2837

76. Hua L, Jiang Y, Li H, Qin L. Effects of different nozzle orifice shapes on water droplet characteristics for sprinkler irrigation. *Hortic* (2022) 8(6):538. doi:10.3390/horticulturae8060538

77. Jiang Y, Chen C, Li H, Xiang Q. Influences of nozzle parameters and low-pressure on jet breakup and droplet characteristics. *Int J Agric and Biol Eng* (2016) 9(4):22–32. doi:10.3965/j.ijabe.20160904.2103

78. Jiang Y, Issaka Z, Li H, Tang P, Chen C. Range formula based on angle of dispersion and nozzle configuration from an impact sprinkler. *Int J Agric and Biol Eng* (2019) 12(5):97–105. doi:10.25165/j.ijabe.20191205.4646

79. Jiang Y, Liu J, Li H, Hua L, Yong Y. Droplet distribution characteristics of impact sprinklers with circular and noncircular nozzles: effect of nozzle aspect ratios and equivalent diameters. *Biosyst Eng* (2021) 212:200–14. doi:10.1016/j.biosystemseng.2021.10.013

80. Wang Z, Jiang Y, Liu J, Li H, Li H. Experimental study on water distribution and droplet kinetic energy intensity from non-circular nozzles with different aspect ratios. *Agriculture* (2022) 12(12):2133. doi:10.3390/agriculture12122133

81. Gong C, Li D, Kang C, Wang Y. Visualisation of the evolution of perforations in oil-based emulsion sheets formed by flat-fan spray nozzles. *Biosyst Eng* (2021) 207:68–80. doi:10.1016/j.biosystemseng.2021.04.005

82. Makhnenko I, Alonzi ER, Fredericks SA, Colby CM, Dutcher CS. A review of liquid sheet breakup: perspectives from agricultural sprays. *J Aerosol Sci* (2021) 157:105805. doi:10.1016/j.jaerosci.2021.105805

83. Yang W, Jia W, Ou M, Zhong W, Jiang L, Wang X. Effect of physical properties of an emulsion pesticide on the atomisation process and the spatial distribution of droplet size. *Agriculture* (2022) 12(7):949. doi:10.3390/agriculture12070949

84. Yang W, Zhong W, Jia W, Ou M, Dong X, Zhang T, et al. The effect of oil-in-water emulsion pesticide on the evolution of liquid sheet rim disintegration and the spraying distribution. *Crop Prot* (2024) 177:106547. doi:10.1016/j.cropro.2023.106547

85. Zhang Y, Jia F, Peng X, Hammad FA, Wang T, Sun K. Impingement of unlike-doublet liquid jets with different surface tensions. *Phys Fluids* (2023) 35(6):061703. doi:10.1063/5.0152701

86. Zhai C, Zhang J, Li K, Dong P, Jin Y, Chang F, et al. Comparative analysis and normalization of single-hole vs. multi-hole spray characteristics: 1st report on spray characteristic comparison. *GER* (2025) 3(1):100120. doi:10.1016/j.gerr.2025.100120

87. Rodrigues NS, Kulkarni V, Gao J, Chen J, Sojka PE. Spray formation and atomization characteristics of non-Newtonian impinging jets at high Carreau numbers. *Int J Multiph Flow* (2018) 106:280–95. doi:10.1016/j.ijmultiphaseflow.2018.05.017

88. An Y, Wang B, Peng Z, Chen X, Yang V. Mechanistic insights and practical applications of impinging-jet dynamics and atomization. *Acta Mech Sin* (2025) 41(7):125469. doi:10.1007/s10409-025-25469-x

89. Ou M, Zhang Y, Wu M, Wang C, Dai S, Wang M, et al. Development and experiment of an air-assisted sprayer for vineyard pesticide application. *Agriculture* (2024) 14(12):2279. doi:10.3390/agriculture14122279

90. Man Y, Zhou C, Adhikari B, Wang Y, Xu T, Wang B. High voltage electrohydrodynamic atomization of bovine lactoferrin and its encapsulation behaviors in sodium alginate. *J Food Eng* (2022) 317:110842. doi:10.1016/j.jfoodeng.2021.110842

91. Pan X, Jiang Y, Li H. Effects of the depth of the needle-shaped water dispersion device inserted into the jet on the jet breakup of sprinklers. *Irrig Drain* (2023) 72(4):887–909. doi:10.1002/ird.2825

92. Pan X, Jiang Y, Li H, Hui X, Xing S, Chauhdary JN. Numerical simulation and experimental study of jet breakup using a water dispersal needle in irrigation sprinklers. *Biosyst Eng* (2024) 239:49–67. doi:10.1016/j.biosystemseng.2024.01.017

93. Dias GS, Machado DA, de Andrade JC, de Souza Costa F. Experimental study of impinging jets of gelled and liquid fluids. *Int J Multiph Flow* (2023) 165:104478. doi:10.1016/j.ijmultiphaseflow.2023.104478

94. Zhang Z, Chi Y, Shang L, Zhang P, Zhao Z. On the role of droplet bouncing in modeling impinging sprays under elevated pressures. *Int J Heat Mass Transfer* (2016) 102:657–68. doi:10.1016/j.ijheatmasstransfer.2016.06.052

95. Zhang Z, Zhang P. Cross-impingement and combustion of sprays in high-pressure chamber and opposed-piston compression ignition engine. *Appl Therm Eng* (2018) 144:137–46. doi:10.1016/j.applthermaleng.2018.08.038

96. Shao S, Ma L, Li X, Zhang H, Xiao R. Preparation of activated carbon with heavy fraction of bio-oil from rape straw pyrolysis as carbon source and its performance in the aldol condensation for aviation fuel as carrier. *Ind Crop Prod* (2023) 192:115912. doi:10.1016/j.indcrop.2022.115912

97. Shao S, Sun T, Li X, Wang Y, Ma L, Liu Z, et al. Preparation of heavy bio-oil-based porous carbon by pyrolysis gas activation and its performance in the aldol condensation for aviation fuel as catalyst carrier. *Ind Crop Prod* (2024) 218:118963. doi:10.1016/j.indcrop.2024.118963

98. Heister S. Pintle injectors. In: *Handbook of atomization and sprays*. Heidelberg, Germany: Springer (2011). p. 647–55.

99. Xu S, Guo G, Yang K, Yuan J, Guan W, Jin Y, et al. Evaluation of a liquid–vapor mass transfer model for string cavitation inside the liquid nozzle with non-condensable gas effects. *Phys Fluids* (2025) 37(5):053329. doi:10.1063/5.0268131

100. Payri F, Bermúdez V, Payri R, Salvador F. The influence of cavitation on the internal flow and the spray characteristics in diesel injection nozzles. *Fuel* (2004) 83(4-5):419–31. doi:10.1016/j.fuel.2003.09.010

101. Yu G, Li G, Wang C. Pressure pulsation characteristics of agricultural irrigation pumps under cavitation conditions. *Water* (2023) 15(24):4250. doi:10.3390/w15244250

102. An C, Liu L, Luo H, Zhou B, Liu Y, Li X, et al. Threshold sensitivity study on spray–spray impingement under flexible injection strategy for fuel/air mixture evaluation. *Phys Fluids* (2025) 37(6):065124. doi:10.1063/5.0268946

103. Li B, Wang Q, Dai L, He Z. Numerical study on combustion and emission characteristics of a dual-fuel direct injection marine engine using ammonia/DME mixtures. *Appl Therm Eng* (2025) 263:125383. doi:10.1016/j.applthermaleng.2024.125383

104. Eli-Chukwu NC. Applications of artificial intelligence in agriculture: a review. *Eng Technol Appl Sci Res* (2019) 9(4):4377–83. doi:10.48084/etasr.2756

105. Jha K, Doshi A, Patel P, Shah M. A comprehensive review on automation in agriculture using artificial intelligence. *AI Agric* (2019) 2:1–12. doi:10.1016/j.aiia.2019.05.004

106. Liu SY. Artificial intelligence (AI) in agriculture. *IT Prof* (2020) 22(3):14–5. doi:10.1109/mitp.2020.2986121

107. Preite L, Vignali G. Artificial intelligence to optimize water consumption in agriculture: a predictive algorithm-based irrigation management system. *Comput Electron Agric* (2024) 223:109126. doi:10.1016/j.compag.2024.109126